Journal of Hydrology 596 (2021) 126088

Contents lists available at ScienceDirect

Journal of Hydrology

journal homepage: www.elsevier.com/locate/jhydrol

Research papers

Understanding the effects of Digital Elevation Model resolution in urban fluvial flood modelling

Manoranjan Muthusamy [a], Mónica Rivas Casado [a,*], David Butler [b], Paul Leinster [a]

[a] School of Water, Energy and Environment, Cranfield University, Cranfield MK430AL, UK
[b] Centre for Water Systems, College of Engineering, Mathematics and Physical Sciences, University of Exeter, Harrison Building, Streatham Campus, North Park Road, Exeter EX4 4QF, UK

ARTICLE INFO

This manuscript was handled by Andras Bardossy, Editor-in-Chief, with the assistance of Jie Chen, Associate Editor

Keywords:
Digital Elevation Model
Resolution
Fluvial flood
Urban flood
Flood extent
Flood depth

ABSTRACT

With the extensive use of 2D flood models, the resolution and quality of Digital Elevation Models (DEMs) have come under greater focus especially in urban hydrology. One of the major research areas, in this regard, is the effect of DEM resolution on flood modelling. This study first investigates the root causes of the impact of DEM resolution on urban fluvial flood modelling outputs using DEMs with grid resolutions ranging from 1 m to 50 m. The study then investigates how DEM resolution affects the definition and characterisation of the river channel and the consequences of this for the modelled results. For this purpose, a separate set of merged DEMs was generated where the river channel as defined by the 1 m resolution DEM is merged with coarser resolution DEMs. Data obtained during the flood event caused by Storm Desmond (2015) in Cockermouth (Cumbria, UK) was used for this study. The HEC-RAS 2D model was used for all of the simulations. The benchmark model obtained with the 1 m resolution DEM was calibrated using measured water levels at two locations within the rivers. Results show that there is a 30% increase in flood extent from 58.9 ha to 79.0 ha and a 150% increase in mean flood depth from 1.74 m to 4.30 m when the resolution reduces from a 1 m grid to a 50 m grid. The main reason for this is the increasing lack of definition of the river channel with an associated reduction in the estimated depth of the river resulting in reduced river channel conveyance. This then leads to an increase in the flood extent and depth especially in the immediate vicinity of the river. This effect is amplified when the DEM grid size is greater than the river width. When the 1 m resolution DEM for the river channel is used in conjunction with coarser resolution DEMs for the surrounding areas (merged DEMs), there is a significant improvement in the agreement between the modelled and the reference case (obtained from the benchmark model) flood extents and depths. The use of merged DEMs reduces the error in mean flood depth from 90% to 4% and reduces the overall RMSE in flood depths from 2.6 m to 0.9 m at 30 m resolution. The use of merged DEMs, where a higher resolution DEM is used to characterise the river channel in conjunction with, for example, a 30 m resolution DEM (e.g., the freely available NASA Shuttle Radar Topography Mission DEMs) for the wider area could be a cost-effective solution for locations where higher resolution DEMs may not be available.

1. Introduction

Between 1998 and 2017, floods affected more than two billion people worldwide and flood together with storms and droughts contributed to 80–90% of the worldwide natural disasters in the last ten years (WHO, 2020). Across England, the Environment Agency (EA) estimates that there are 2.7 million properties at risk of fluvial and coastal flooding, three million properties at risk of pluvial flooding and 660,000 at risk from all sources (coastal, fluvial and pluvial) (Environment Agency, 2009). With the ever-increasing development of dwellings on flood plains (Pottier et al., 2005) and more extreme and intense rainfall events due to phenomenon such as El Niño driven by global warming (Corringham and Cayan, 2019; Ward et al., 2014), the frequency, magnitude and impacts of flood events are only going to increase. Accurate modelling and forecasting of flooding play a major role in the better management of flood risk. The rapid advancement in remote sensing data collection and monitoring over the last decade has facilitated more widespread flood modelling activities (Bates, 2012, 2004; Schumann et al., 2009, 2007). For example, NASA's Shuttle Radar Topography Mission (SRTM) has provided a 30 m resolution Digital

* Corresponding author.
E-mail address: casado@cranfield.ac.uk (M.R. Casado).

https://doi.org/10.1016/j.jhydrol.2021.126088
Received 26 January 2021; Received in revised form 26 January 2021; Accepted 13 February 2021
Available online 20 February 2021

Elevation Model (DEM) globally for free from 2015. In addition, many countries have their own databases of DEMs with higher resolution than the SRTM 30 m resolution data. For example, within England, digital terrain models (DTMs) and digital surface models (DSMs) of 1 m resolution are available at no cost from the EA (Environment Agency, 2018). This wide availability of Digital Elevation Models (DEM) together with supercomputers to handle the required simulation power has made 2D flood modelling the preferred option for predicting flood properties including extent, depth and velocity, especially in urban areas where surface dynamics are very high. With the extensive use of 2D flood models, the resolution and quality of DEMs have come under greater focus especially in urban hydrology (Ogania et al., 2019; Ozdemir et al., 2013; Peña and Nardi, 2018; Saksena and Merwade, 2015a). One of the major research areas, in this regard, is the effect of DEM resolution on the estimation of flood properties. It is perhaps obvious that higher resolution DEMs produce more accurate results as long as the model can handle such high resolution DEMs. However, with so many financial and practical challenges in producing a wide area high-resolution DEM (<1m) especially in developing countries and the associated computational burden, it is not necessarily the highest resolution DEM, but the optimal resolution DEM, that is to be preferred (Azizian and Brocca, 2020; Brandt, 2016).

Although the optimal resolution for a particular area and application will depend on the catchment characteristics, common criteria can be identified by investigating the DEM resolution vs flood characteristics relationship in detail for various catchment and flood types. For example, Saksena and Merwade (2015) analysed a range of DEM resolutions from 6 m to 30 m in fluvial flood modelling and sought to relate the differences arising from the use of the various DEM resolutions with the resultant flood inundation maps. They then used this information to create improved flood inundation maps from coarser-resolution DEMs. They found that increasing the grid size of the DEM increased the flood areas and flood depths. However, application of this finding is limited to fluvial flooding and to the specific catchment characteristics and cannot be generalised to all catchment types. In fact, most of the studies, which suggest that coarser-resolution DEMs result in the overprediction of flood areas and/or flood depths are based on fluvial modelling. Over time, this has resulted in a common perception that regardless of flood type coarser-resolution DEMs will always result in an overprediction of flood extent and depth.

However, studies also show the opposite behaviour when it comes to surface water flooding. Ozdemir et al. (2013) found that when the DEM resolution is increased from 1 m to 10 cm the resultant maximum flood depth increases. However, this resolution range was used to identify the impacts of micro-urban surface dynamics such as small bumps in the road and cannot be generalised over a wider area, in which the surface dynamics are predominately due to larger structures and buildings. There are also studies, which show an inconsistent pattern of flood properties against DEM resolution (Tamiru and Rientjes, 2005).

This inconsistency in the results and conclusions of previous studies demands a more detailed analysis, which should not only focus on the results but also investigate the root cause of the differences observed. This will help to build a common understanding of the effect of DEM resolution on flood properties. Such in-depth analysis is lacking in most of the previous studies and some of the studies identified the need for further in-depth analysis (Tamiru and Rientjes, 2005). All the studies above, which investigated the effect of DEM resolution, used a uniform resolution for the whole area during any particular model run. This makes it difficult to pinpoint the root cause of the behaviour of the flood model especially when there is a river or canal present in the model area. The effect of a coarser-resolution could be different depending on the land use - for example, a river and a developed area will exhibit different behaviours in terms of flood propagation when studied using different resolution DEMs. When a uniform resolution DEM is used over the entire study area, it is difficult to pinpoint the root cause of over/under prediction resulting from a coarser resolution DEM.

This study aims to investigate the effect of DEM resolution in the definition and characterisation of the river channel and the consequences of this in urban fluvial flood modelling by making use of a merged DEM approach with different resolutions for river and the rest of the area. The objectives are to (a) examine the effect of DEM resolution on flood depth and flood extent, (b) investigate the root cause of the effect and (c) find out whether improving the definition of the river channel by using the merged DEM significantly affects the predicted outcomes for flood extent and depth.

2. Methodology

2.1. Study site and selected flood event

The study site, Cockermouth is a market town located at the confluence of the rivers Cocker and Derwent in the Northwest of England (Cumbria, UK). It covers approximately 142 ha (Fig. 1). According to the 2011 census data, the town has a population of around 8800 people and 4000 households. The River Cocker is a tributary of the River Derwent and flows for 19 km before joining the Derwent in Cockermouth (2011) (Office for National Statistics, 2018). The maximum river widths of the rivers within the study site are approximately 15 m and 50 m for the River Cocker and the River Derwent, respectively. The study area represents a typical urban area with a large proportion of built-up area as can be seen from Fig. 1. Furthermore, since the lowest resolution used in this study was 1 m, it was a preferable choice to use a small urban area for this study as it allows us to understand the local DEM and flood dynamics better as demonstrated in previous studies (e.g. Leitão et al., 2016; Ozdemir et al., 2013). Cockermouth has experienced serious flood events in 2005, 2009 and 2015. In 2015 the town was severely affected by three consecutive storms: Desmond (5–6/12/2015), Eva (24/12/2015) and Frank (29–30/12/2015) (Met Office, 2018). Storm Desmond resulted in record-breaking rainfall of 341.4 mm and 405 mm over 24 hrs and 48 hrs respectively. It resulted in severe flooding with 5200 homes in the northeast of England (Met Office, 2018) being impacted. A peak flow of between 390 m^3/s – 450 m^3/s was recorded on the River Derwent at Ouse Bridge. This exceeded the previous highest peak flow ever recorded (378 m^3/s). Due to the national level significance of this event, this event was well documented which is one of the reasons for the selection of this case study.

2.2. Data collection

The topographical and hydrological data used in this study (Table 1) were all obtained from the EA (Environment Agency, 2009). As stated previously, high-resolution DTM and DSM up to 25 cm resolution are available for England at no cost from the EA. All the DEM used in this study were derived from the 1 m DSM and DTM. Volumetric flow at the river boundaries of the model domain was not available. However, volumetric flow time series were available for both rivers at 15 min intervals at Southwaite Bridge and Ouse Bridge for the River Cocker and River Derwent respectively, which are located considerably farther from the modelled river boundaries. This data was used in this study for boundary conditions with necessary adjustment, which is explained in detail in section 2.3. As Cockermouth is situated at the confluence of two rivers and also due to frequent flooding at Cockermouth, there are two water level gauging stations on the rivers, located at P1(River Cocker) and P2 (River Derwent) as indicated in Fig. 1. This data was used for the calibration of the fluvial flood model.

2.3. Flood inundation modelling

2.3.1. DEM generation

A DEM of the study site at 1 m resolution was generated using the DSM and DTM obtained from the EA. The river channels were extracted from the DTM and placed in the DSM to obtain the river depths. Once the

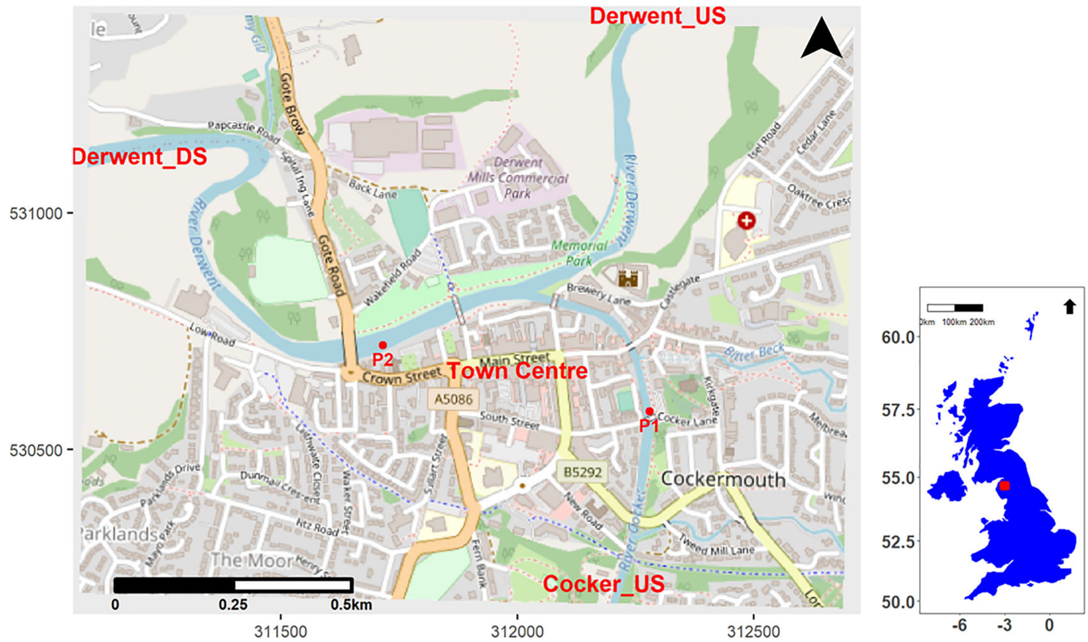

Fig. 1. Study Site in the town of Cockermouth showing the two rivers (River Cocker and River Derwent), town centre and river boundaries, Cocker upstream boundary (Cocker_US), Derwent upstream boundary (Derwent_US) and Derwent downstream boundary (Derwent_DS). P1 (River Cocker) and P2 (River Derwent) are calibration points where water levels measurements were taken. (Copyright statement - © OpenStreetMap contributors CC-BY-SA).

Table 1
Summary of data collection.

Data type	Source	Resolution and accuracy if available	Details
DSM and DTM	EA	1 m resolution Vertical error = +/−15 cm root mean square error (RMSE). Horizontal error = +/−40 cm absolute error (this error is effectively absorbed in the pixels of the raster image)	Generated using the composite of a merge of datasets from differing resolutions (made up of resampled 25 cm and 50 cm surveys as well as 1 m surveys) collected from 2010 to 2015. These data were collected using the Light Detection and Ranging (LiDAR) sensor.
Boundary conditions	EA	15 min	The upstream volumetric flows for the River Cocker and the River Derwent from 03/12/2015 to 09/12/2015. Derived from stage curves.
Calibration data	EA	15 min	River water levels at points P1 and P2 (Ref. Fig. 1) from 03/12/2015 to 09/12/2015

1 m resolution DEM was generated, it was then resampled to produce coarser DEMs with 2 m, 5 m, 10 m, 30 m and 50 m resolutions. Except for the 30 m resolution which represents freely available SRTM data, other resolutions were chosen to represent a range of potentially useful DEM resolutions. These DEMs are presented in Fig. 2. Using the range of DEMs produced, a second set of DEMs were generated where the river channel of each of the DEMs was replaced with the river channel from the 1 m resolution DEM. In the following sections, the DEMs with the river channels at the same resolution as the rest of the surveyed area are referred to as 'uniform DEMs' and those where the river channel is based on a 1 m resolution DEM and the rest of the surveyed area is based on a range of DEM resolutions are referred to as 'merged DEMs'.

2.3.2. *Flood modelling*

The 2D flood inundation modelling was carried out using HEC-RAS (v5) 2D (U.S. Army Corps of Engineering, 2016). HEC-RAS 2D is capable of simulating surface flooding caused by rainfall as well as river flooding (U.S. Army Corps of Engineering, 2016). In this study, we only analysed the fluvial flooding resulting from both rivers. Pluvial flooding was not modelled. HEC-RAS (v5) 2D provides a means of creating 2D terrains with multiple resolutions which made it possible to run the model with merged DEMs. HEC-RAS 2D solves either the full 2D Saint Venant equations or the 2D diffusive wave equations as described below (U.S. Army Corps of Engineering, 2016):

$$\frac{\partial \zeta}{\partial t}+\frac{\partial p}{\partial x}+\frac{\partial q}{\partial y}=0 \tag{1}$$

$$\frac{\partial p}{\partial t}+\frac{\partial}{\partial x}\left(\frac{p^2}{h}\right)+\frac{\partial}{\partial y}\left(\frac{pq}{h}\right)=-\frac{n^2pg\sqrt{p^2+q^2}}{h^2}-gh\frac{\partial \zeta}{\partial x}+pf+\frac{\partial}{\rho\partial x}(h\tau_{xx})+\frac{\partial}{\rho\partial y}(h\tau_{xy}) \tag{2}$$

$$\frac{\partial q}{\partial t}+\frac{\partial}{\partial y}\left(\frac{q^2}{h}\right)+\frac{\partial}{\partial x}\left(\frac{pq}{h}\right)=-\frac{n^2qg\sqrt{p^2+q^2}}{h^2}-gh\frac{\partial \zeta}{\partial y}+qf+\frac{\partial}{\rho\partial y}(h\tau_{yy})+\frac{\partial}{\rho\partial x}(h\tau_{xy}) \tag{3}$$

where h is the water depth (m), p and q are the specific flow in the x and y directions ($m^3\ s^{-1}$), is the surface elevation (m), g is the acceleration due to gravity ($m\ s^{-2}$), n is the Manning roughness, $\rho$is the water density ($kg\ m^{-3}$), τ_{xx}, τ_{yy} and τ_{xy} are the components of the effective shear stress and f is the Coriolis (s^{-1}). Equation (1) is the continuity equation and Eqs. (2) and (3) are the momentum equations in the x and y-axis respectively. Together these equations are referred to as 2D Saint Venant equations. When the diffusive wave is selected, the inertial terms of the momentum equations (Eqs. (2) and (3)) are neglected and the resulting set of equations are called the 2D diffusive wave equations.

HEC-RAS 2D fluvial flooding requires two main inputs – DEM and river boundary conditions. There are two upstream boundaries (Cocker_US and Derwent_US in Fig. 1) and one downstream boundary

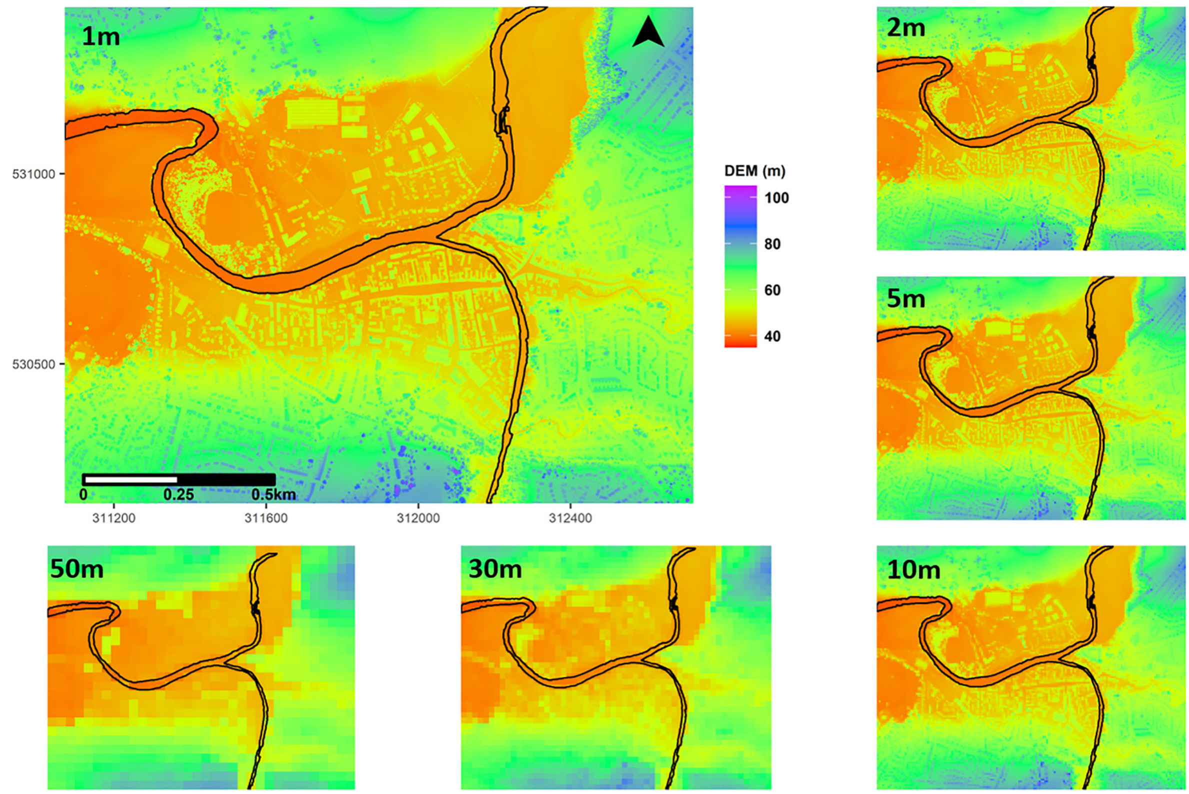

Fig. 2. Uniform DEMs of the study area at resolutions of 1 m, 2 m, 5 m, 10 m, 30 and 50 m. The coarser resolution DEMs (2 m–50 m) were derived by resampling the 1 m DEM. River boundaries are highlighted in black. (Copyright statement: contains public sector information licensed under the Open Government Licence v3.0).

(Derwent_DS) in the model domain. Since there were no observed data available at the downstream boundary, a normal depth condition calculated based on the energy slope was used. Despite the lack of observed data at this location, the boundary condition adopted provides a semi-dynamic condition (i.e. as the flow changes, so does the downstream boundary depth). The input required by the HEC-RAS 2D model for this boundary condition is the energy slope calculated at the downstream point, which in our case was 0.1. Measured volumetric flow time series were available for both rivers at 15 min intervals at Southwaite Bridge and Ouse Bridge for the River Cocker and River Derwent respectively, which are located considerably farther from modelled river boundaries (Cocker_US and Derwent_US in Fig. 1). The quantity of data and the time needed to model the entire extent of both rivers using the measured boundary points meant this was not feasible. We did not use a routing model for the following reasons:

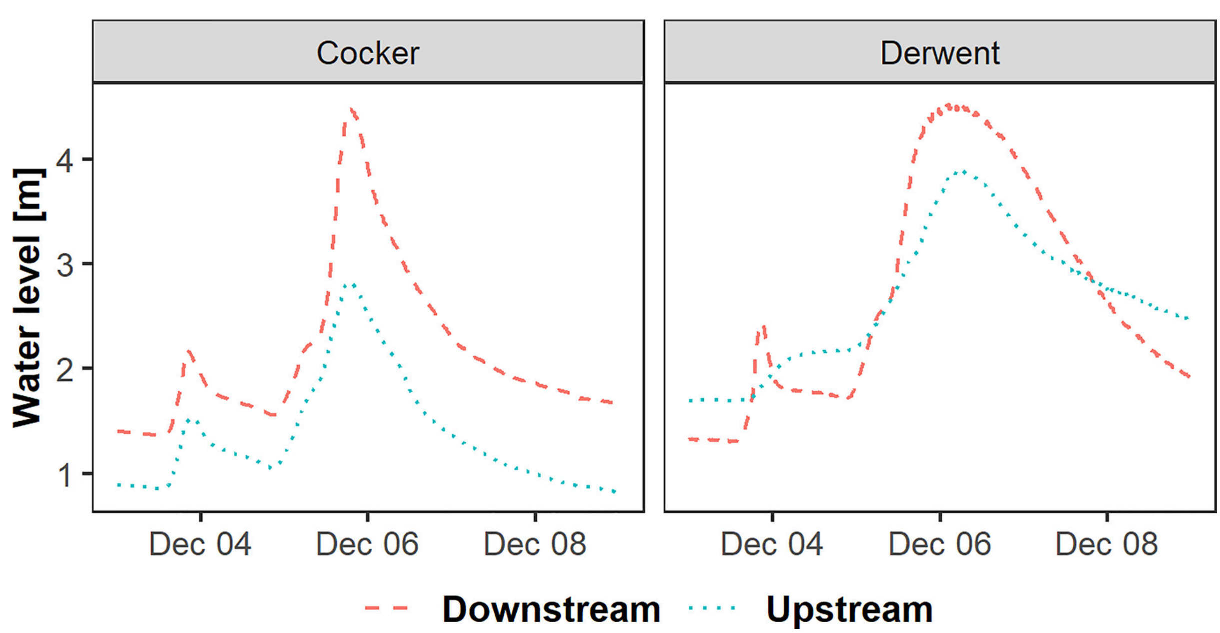

Fig. 3. Water level comparisons between upstream (Southwaite Bridge for the River Cocker and the Ouse Bridge for the River Derwent) and downstream points (P2 for the River Cocker and P1 for the River Derwent).

1. Inadequate river flow data. Flow data for the River Cocker was only available at one location which is Southwaite Bridge. P1 and P2 only provide water level measurements. This did not only constrain the use of a routing model (e.g., Musningkum) for the River Cocker but also affects the impact of the River Cocker on the River Derwent flows when using a routing model for the River Derwent.
2. When comparing the water level data for both the River Cocker and the River Derwent (Fig. 3), we noticed that there is no significant lag in the peaks between the upstream locations (the Southwaite Bridge for the River Cocker and the Ouse Bridge for the River Derwent) and the downstream locations (P1 for the River Cocker and P2 for the River Derwent). The water levels in the River Cocker increased along the measured length without either attenuation in level or a time lag.

Due to the above reasons, we used a simple model to obtain the boundary conditions. As all the analyses were carried out using the maximum flood extent and depths, the main objective of the calibration was to get the modelled peaks of the flood as close as possible to the observed peaks. Hence, we adjusted the measured river flow time series at the Ouse Bridge (for the River Derwent) and at the Southwaite Bridge (for the River Cocker) using a constant multiplier. We started with a multiplier of 1 (no changes) for both boundaries (Cocker_US and Derwent_US). We then adjusted the multiplier for the Cocker_US until a good agreement was obtained between the measured and modelled water levels at P1. A good agreement was obtained using a multiplier of 1.42. Once the Cocker_US boundary condition was fixed, we then adjusted the multiplier for the Derwent_US until a good agreement was at P2. This was obtained using a multiplier 0.96 at the Derwent_US.

For the Manning's coefficient, we followed the approach described in many hydraulic modelling studies in the past (Aronica et al., 2002; Horritt and Bates, 2001; Jung et al., 2012; Savage et al., 2016; Werner et al., 2005) and used two different values - a value of 0.035 (corresponds to major natural rivers) for river channels and a value of 0.05 for the flood plain (i.e. the rest of the area). These values were selected based on the recommended values in widely used literature (e.g. Chow, 1959; Arcement and Schneider, 1989).

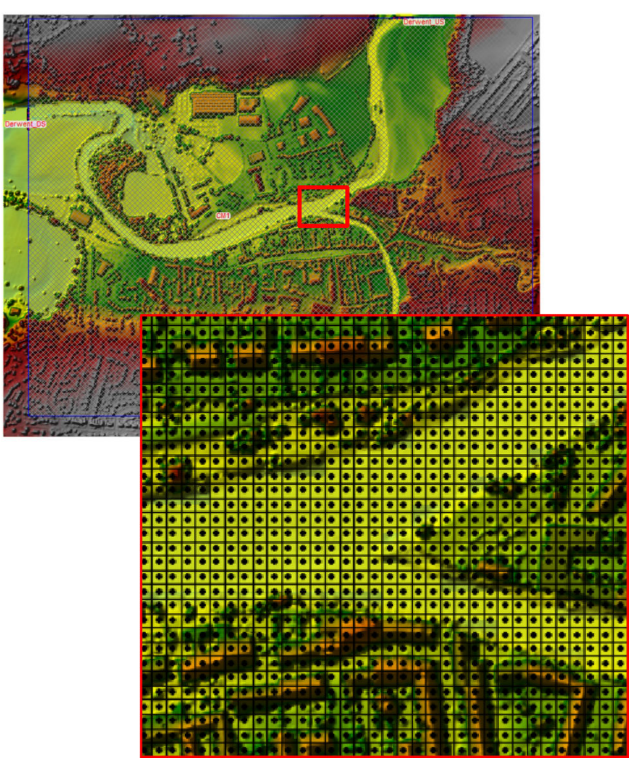

Fig. 4. Mesh used for all simulations with 1 m DEM in the background and zoomed window for a clearer view.

For all the simulations, a computational mesh with 5 m square cells was used (Fig. 4). The main aim of this study was to evaluate the effect of DEM resolution. Hence, to avoid the mesh configurations affecting the model results, we kept the mesh configuration consistent for all simulations with different configurations of DEM.

2.4. *Fit index analysis*

In order to compare the results from different resolution DEMs and also to compare the effect of the composition of the DEMs (uniform or merged), different measures were used. In addition to the common error measure such as Root Means Square Error, we also used a Fit Index (FI) analysis to compare the results. FI is a measure of the error between the reference and predicted flood areas (Horritt and Bates, 2001; Pappenberger et al., 2007). Fig. 5 and equation (4) illustrate the basis of the FI analysis.

$$Fit\ Index(FI) = \frac{A_{Ref} \cap A_{Pre}}{A_{Ref} \cup A_{Pre}} = \frac{A_{TP}}{A_{TP} + A_{FP} + A_{FN}} \quad (4)$$

Essentially, FI varies from 0 when the true positive area is 0 and 1 when there is 100% fit on the basis of flood area between the reference and predicted maps.

3. Results and discussion

3.1. *Goodness-of-fit between the reference model and observations*

3.1.1. *River water levels*

Fig. 6 illustrates the goodness-of-fit between the modelled results obtained using a 1 m DEM and the measured water levels at two locations; the first on the River Cocker (P1) and the second on the River Derwent (P2). Root Mean Square Errors (RMSE) between the measured and simulated water levels were calculated as being 0.28 and 0.69 respectively. The main reason for a better calibration at P1 is because only one boundary has to be adjusted to calibrate at P1 which is located before the confluence of the River Derwent and River Cocker. P2 is located after the confluence of the two rivers and therefore both boundaries had to be adjusted which resulted in a slightly poorer goodness-of-fit. Since the analysis mainly uses maximum flood depths, the emphasis was placed on calibrating the peaks of the hydrograph. The peaks were calibrated with 7% and 1% error at P1 and P2 respectively.

3.1.2. *Flood extent*

We also compared the modelled flood extents with the measured flood extent as provided by the EA (Fig. 7). The EA flood extent was provided with a note stating that the flood outline identifies the maximum extent of flooding and not all properties within the extent were flooded. However, no further information was available to identify the areas within the overall extent that were not flooded. This explains why the EA flood extent is completely filled-in whereas the model predicted flood extent contains many unflooded areas within the maximum extent. However, the outer boundary of the extents is almost similar indicating a good agreement between the modelled and measured flood extents.

As with most floods, there are no measured flood depths available for this event. The calibrated model results obtained with the 1 m DEM are therefore considered to be benchmark conditions (reference case) for all the analysis presented.

3.2. *Flood area and depth: Uniform DEM*

Fig. 8 presents the maximum flood depth maps for different resolutions derived from HEC-RAS 2D results when the uniform DEMs were used in the simulations. The inundated area increases as the resolution of the DEM becomes coarser. The flooded area increased from 59 ha to

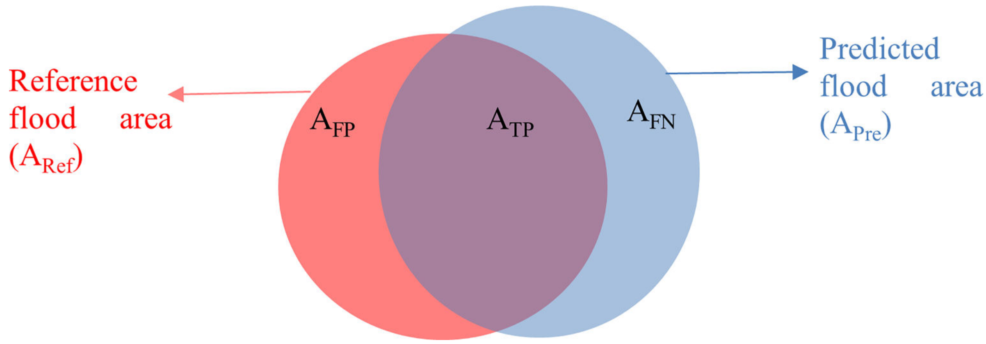

Fig. 5. Illustrative figure showing A_{FP}, A_{TP} and $A_{FN.}$ A_{TP} – True Positive area (Correct prediction); A_{FP} – False Positive area (Underestimation); A_{FN} – False Negative area (Overestimation).

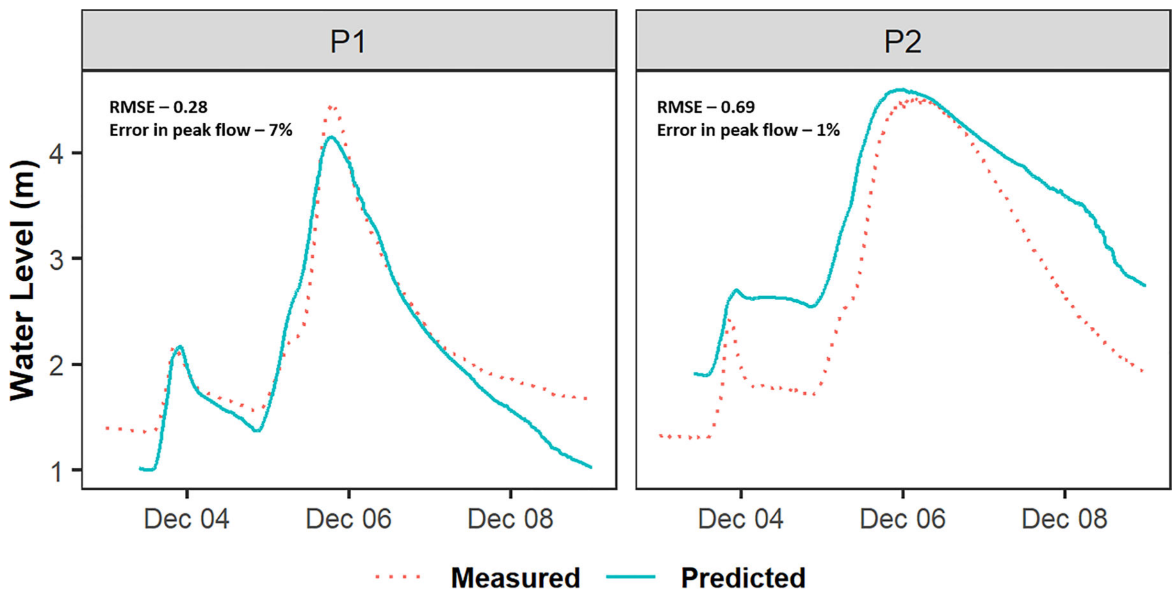

Fig. 6. Calibration plot at location P1 (River Cocker) and P2 (River Derwent). Predicted values are derived from HEC-RAS 2D results with a 1 m DEM.

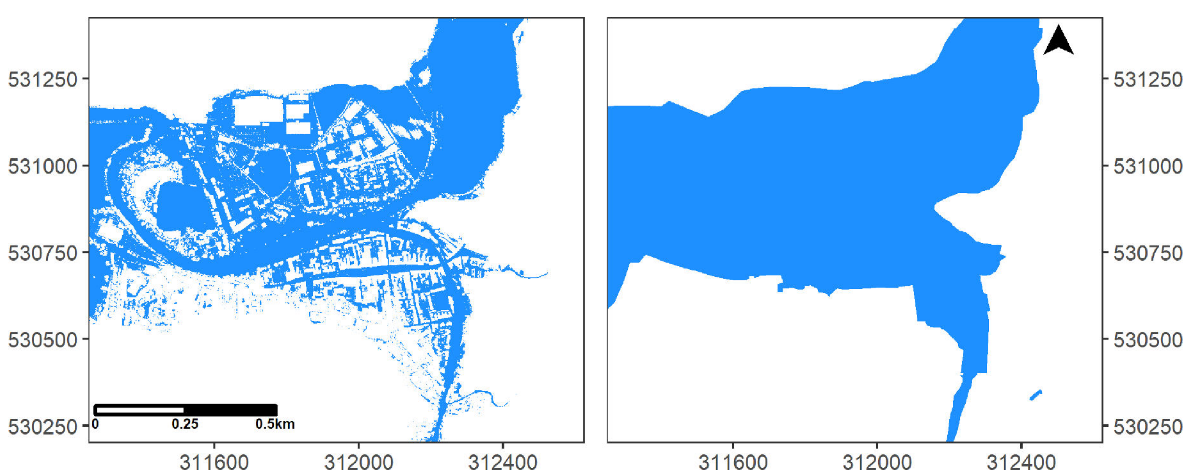

Fig. 7. Comparison between the HEC-RAS simulated flood extent (Left) and measured outer flood extend from the Environment Agency (Right).

79 ha when the resolution went from 1 m to 50 m. Most of the small pockets within a flooded area that are not showing as flooded in the higher resolution simulations due to the surrounding taller buildings/ developments are indicated as having flooded in the lower resolution model runs. In addition, the modelled flood depths generally are higher for the coarser-resolution model runs. Although this effect occurs almost everywhere, it is significantly amplified in the vicinity of the River Cocker. To analyse this effect further, we looked at cross-sections of the two rivers as indicated on Fig. 9 - X-X on the River Derwent and Y-Y on the River Cocker at DEM resolutions of 1 m, 10 m and 50 m. For both cross-sections, at the coarser resolutions, the riverbed becomes smoother and less deep due to the influence of the adjacent riverbanks.

Fig. 8. Flood inundation maps produced using uniform DEMs ranging from 1 m to 50 m.

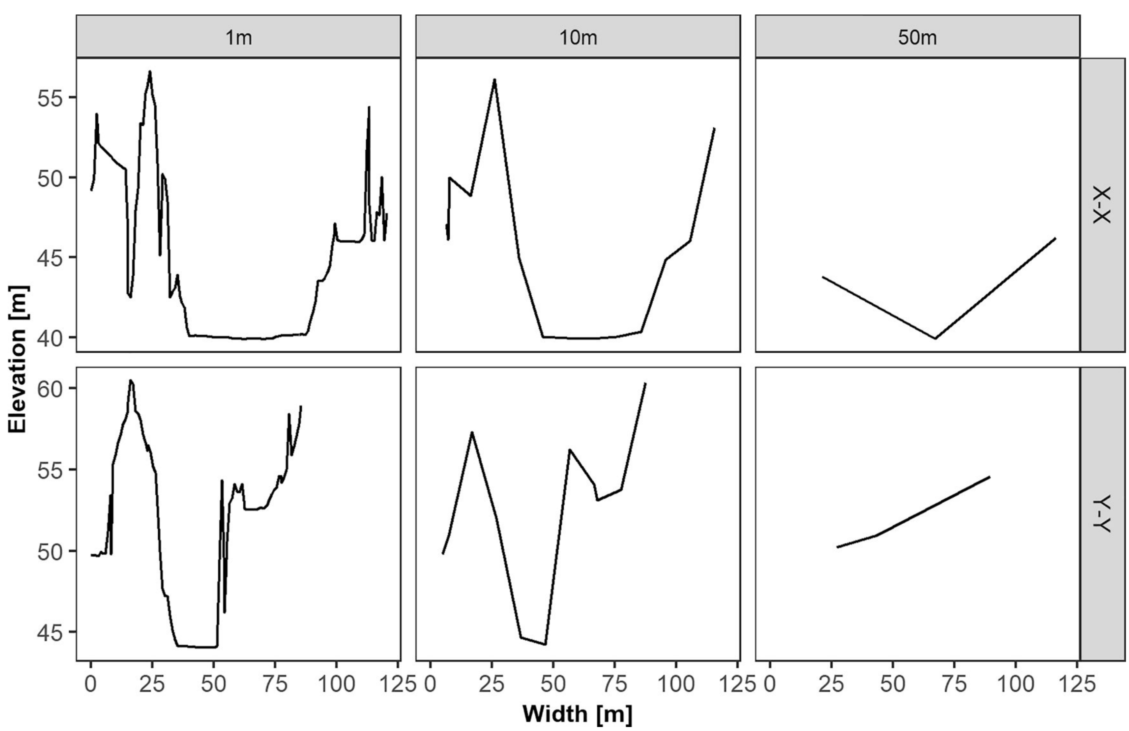

Fig. 9. Cross sections X-X and Y-Y (Fig. 8) for resolutions 1 m, 10 m and 50 m.

In the case of the River Cocker (Y-Y), as the width of the river at this location is only approximately 15 m, the river almost disappears from the simulation when the DEM used is coarser than 10 m. This is reflected in the flood extent and flood depth in Fig. 8 where the flood depth and extent become significantly higher in the vicinity of the River Cocker when the resolution is coarser than 10 m. Flood extent and depths in the vicinity of the River Derwent also increase, but not as significant as for the River Cocker due to the larger river width. Similar observations were observed for cross-sections at other locations along both rivers. However, for the sake of brevity, we have only presented one cross-section from each river here.

We also wanted to check if this increase in flood extent and depth is

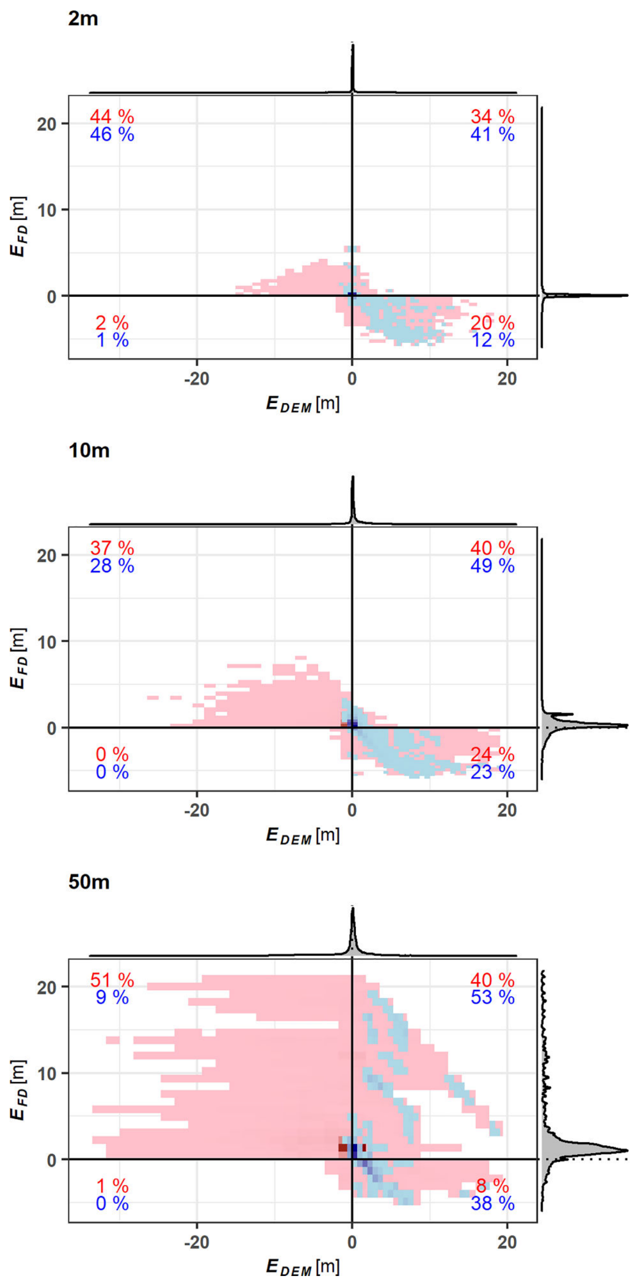

Fig. 10. Binned scatter plots of E_{FD} vs E_{DEM} for DEM resolutions ranging from 1 m to 50 m. The blue colour palate shows cells located in the river and the red colour palate shows the rest of the cells. This figure also shows the density plots of E_{FD} and E_{DEM}, and the percentage of land (red text) and river cells (blue text) that fall in each region of the plot. (For interpretation of the references to colour in this figure legend, the reader is referred to the web version of this article.)

only due to differences in the depth of the riverbed or if other factors contributed to this – for example, taller buildings being smoothed out as a result of a coarser-resolution DEM could also result in a larger flood extent. However, this could also result in the opposite effect with the coarser-resolution raising certain cells due to smoothing which could then become a barrier to the floodwater propagating to other cells. To see how a change in DEM resolution affects the apparent flood depth, we plotted the change in the flood depth (E_{FD}) of a flooded cell against the change in the elevation (E_{DEM}) of that cell for each flooded cell and repeated this for all resolutions (Fig. 10).

E_{FD} and E_{DEM} are defined in Eq. (5) and Eq. (6) repectively

$$E_{FD_i^j} = FD_i^j - FD_r^j \quad (5)$$

$$E_{DEM_i^j} = DEM_i^j - DEM_r^j \quad (6)$$

where FD is flood depth, DEM is elevation, Subscripts i indicates the resolution of interest (2 m, 5 m, 10 m, 30 m and 50 m), r indicates the reference resolution (i.e. 1 m) and superscript j indicates the particular cell of interest. Since, E_{FD} and E_{DEM} are essentially the differences from the reference condition, in the following sections they are also referred to as the error in flood depth and error in the elevation respectively.

The authors are aware that the difference in the flood depth in a cell is also affected by the surrounding cells. Understanding these dynamics across the model domain is of great interest in modelling but are difficult to define and generalise. Hence, we limited this analysis to the effect of the elevation difference in the particular cell of interest. The results are presented in Fig. 10 where two colour pallets are used - blue for cells located within the river area (hereafter referred to as river cells) and red for other locations (hereafter referred to as land cells). Fig. 10 also shows the density plots of E_{FD} and E_{DEM}, and the percentage of land (red numbers) and river cells (blue numbers) that fall in each region of the plot.

The distribution of E_{DEM} – There is an increasing spread of E_{DEM}, demonstrating a greater error as the DEM becomes coarser. For the land cells, the change in the DEM is almost equally distributed in terms of an increase (positive E_{DEM}) and a decrease (negative E_{DEM}) in relation to the benchmark for all the coarser resolutions. This means the coarser-resolution DEM raised as many land cells as it lowered. With the river cells, at 2 m resolution, the effect is similar to that for the land cells with E_{DEM} distributed almost equally in both sides of the axis. However, as the DEM becomes coarser, the proportion of cells indicating values lower than the benchmark keeps decreasing and when the resolution is more than 30 m it becomes less than 10%. Both river beds are higher than the reference DEM due to the influence of the river banks when the DEM resolution is more than 10 m. In summary, we found that as the DEM resolution becomes coarser i) there are equal increases and decreases in the modelled elevation of individual land cells and ii) the majority of the river cells are elevated due to the influence of the river banks.

The correlation between E_{FD} and E_{DEM} – The increased overflow from the river, resulting from the reduction in the channel definition, caused an increase in the indicated flood depths (positive E_{FD}) of 76–92% of the cells. Among these are almost all of the cells which decrease in height due to the coarser resolution (negative E_{DEM}). The remaining 8–24% cells which indicate a reduced flood depth are all cells which increase in height at coarser resolutions.

The flood depth of the majority of river cells increases (positive E_{FD}) when using a coarser resolution DEM. However, it can be seen that there are river cells with positive E_{DEM} and negative E_{FD} - meaning the raised river bed causes a reduction in the flood depths for a proportion of river cells. The proportion of river cells with a positive E_{DEM} and negative E_{FD} increases from 11% to 39% when the resolution changes from 2 m to 50 m. These river cells are mostly located at locations where there are no barriers such as tall buildings in the flood plain. This allows the floodwater to propagate out of the river reducing the flood depth of raised river cells. To illustrate this, we have presented a cropped area of the flood map obtained using a 50 m resolution DEM in Fig. 11 indicating areas with a negative and a positive E_{FD} together with a road map of the same area. It can be seen that the raised river cells with an increased flood depth (positive E_{FD}) are located along a stretch of river where it is surrounded by a highly developed area, with tall buildings, which confine the flow resulting in the higher flood depths of river cells. In contrast, raised river cells with decreased E_{FD} are located along a stretch of river where it is surrounded by a low-lying undeveloped area which lets the flow propagate out of the river. It is therefore important to note that although the coarser-resolution DEM invariably raises the river bed, it doesn't always result in an increase in the flood depth within the river cells.

Finally, when using the 30 m and 50 m resolution DEMs, as can be seen in Fig. 9, the lack of definition of the river channel and the banks, especially for the River Cocker results in very high modelled flood depths. It is recognised that some of these modelled depths, of up to 20 m, for both river and surrounding land cells are not credible in reality.

3.3. Flood area and depth: Uniform DEM vs merged DEM

Having examined the effect of resolution on uniform DEMs, this section examines what happens if a merged DEM is used instead of a uniform DEM. Fig. 12 shows flood maps for resolutions of 10 m, 30 m and 50 m for both uniform and merged DEMs. The visual difference between the flood maps with merged and uniform DEMs for resolutions less than 10 m is not obvious, so for the sake of brevity, we have not included these plots. However, the results from these DEMs are included in the numerical analyses that are presented later.

Flood maps based on a merged DEM provide a better agreement with the baseline 1 m resolution map in terms of both flood extent and flood depth mainly due to the unchanged riverbeds compared with the uniform DEM approach. However, there was no consistent trend of over-estimation or underestimation in flood extent. As we observed in Fig. 10, the changes in the elevation of land cells due to coarser resolution are random, so consequently, the effect caused by these random elevation

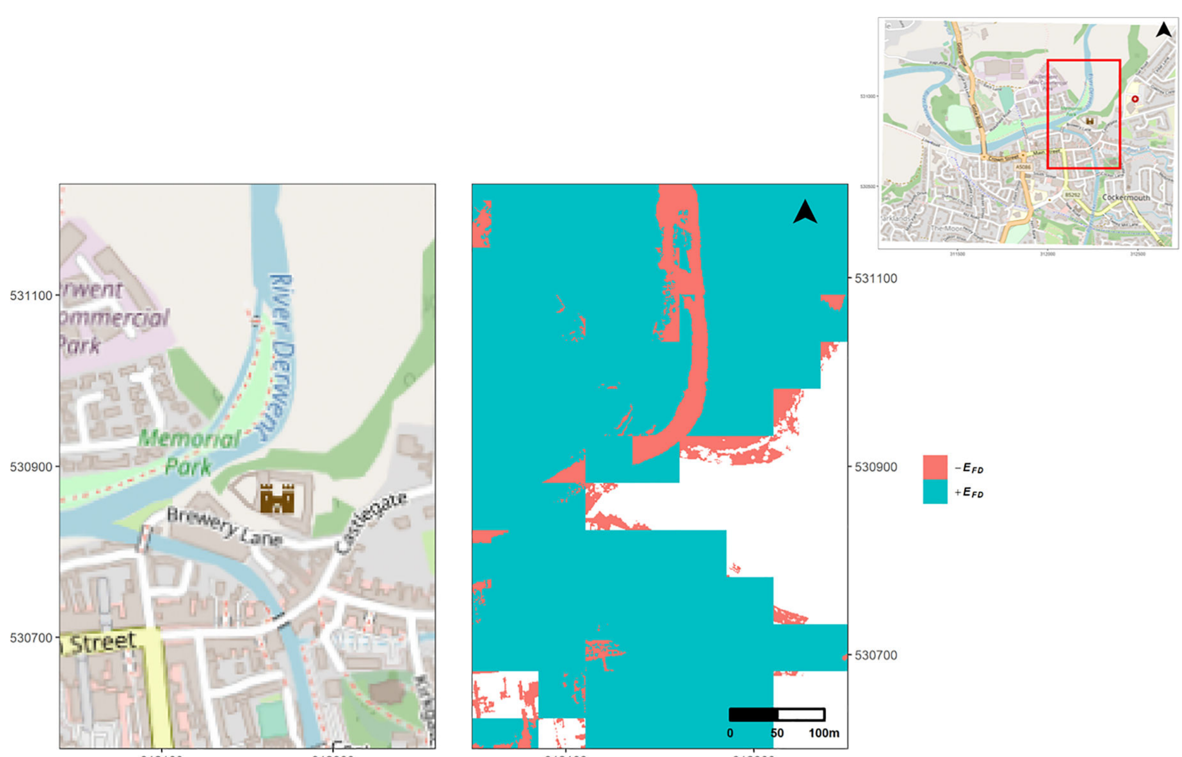

Fig. 11. Right: Cropped area of the street map (Copyright statement- © OpenStreetMap contributors CC-BY-SA). Left: Cropped area of flood map with 50 m resolution DEM showing positive and negative E_{FD}.

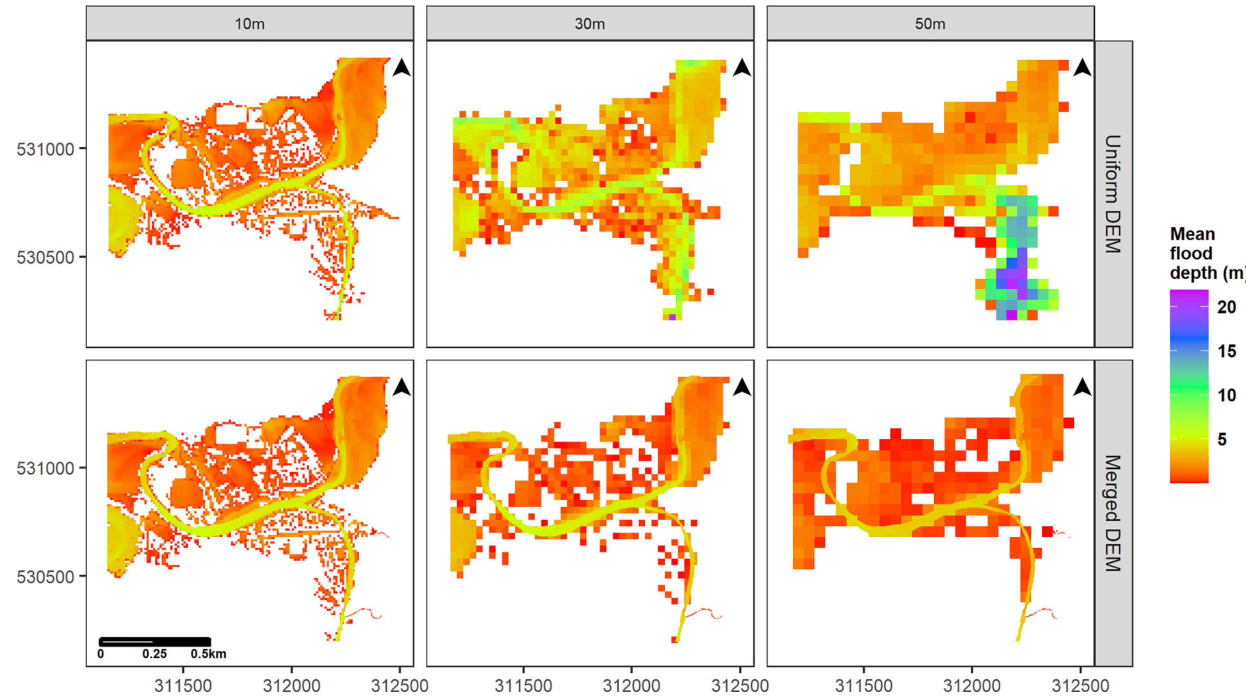

Fig. 12. Flood inundation maps produced using uniform and merged DEMs for resolutions 10 m 30 m and 50 m.

changes in the flood properties are also expected to be random without the overbank flood caused by the river. Flood maps with a merged DEM and resolutions of 30 m and 50 m failed to predict many small pockets of flooding resulting in an underestimation of the flooded area. One reason could be that low-lying small passages in the developed areas, which aid flood propagation, are now elevated in the coarser-resolution DEMs (30 m and 50 m) due to surrounding buildings and therefore do not propagate the flood to neighbouring locations anymore. Hence, the increase or decrease of the flooded area with decreasing resolution in a merged DEM is highly dependent upon the local terrain characteristics and there is no consistent trend in contrast to the trend that was apparent with the uniform DEM approach.

Fig. 13 shows the distribution of flood depths derived using the uniform and merged DEMs together with vertical dotted lines showing the average flood depth. It can be seen that there is greater consistency in estimation compared with the 1 m resolution DEM reference case when using the merged DEM approach in terms of the average depth and distribution. As the resolution of the uniform DEM decreases the distribution becomes smoother and wider with an increase in the estimated mean value. At 50 m resolution, the error in mean flood depth is ~150%. However, when using the merged DEM approach, the greatest difference is ~20% and this was again obtained in the case of the 50 m resolution DEM. There is a significant difference in both the shape of the distribution and the mean flood depth when the uniform DEM resolution changes from 10 m to 30 m. This is due to the width of the river channels (River Cocker ~15 m, River Derwent ~50 m) in relation to the resolution of the DEM. At 1 m resolution (reference flood depths), there are two peaks corresponding to cells from each river (and the surrounding cells). This characteristic of the distribution is better matched when using the merged DEM approach even when the resolution is 50 m.

The changes in the indicated flood area for the various DEM resolutions are presented in Fig. 14 and Table 2 for both uniform and merged DEMs. In Fig. 14, the area of land flooded above the threshold depth was calculated for threshold flood depths ranging from 0 (all flooded area) to 5 m. In the case of the uniform DEMs, the decrease in the DEM resolution

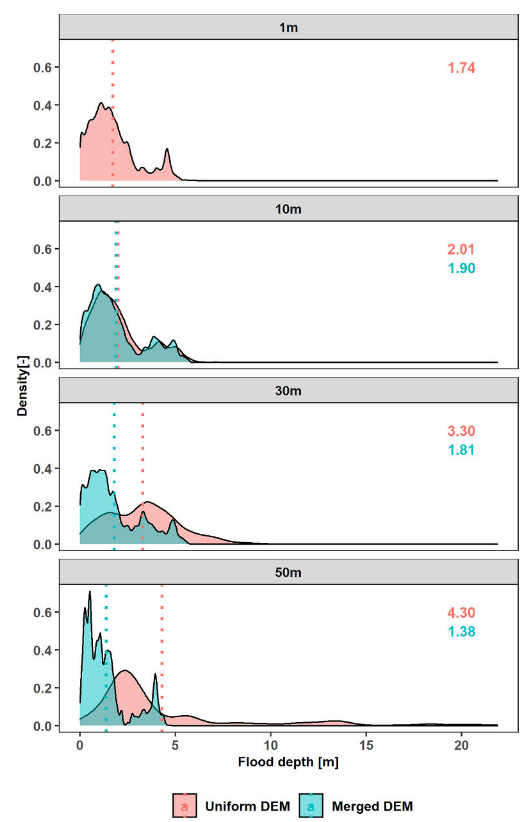

Fig. 13. Distribution of flood depth across the model domain for both uniform and merged DEMs ranging from 1 m to 50 m. The mean of the distribution is indicated with dotted lines and also presented as text with corresponding colour.

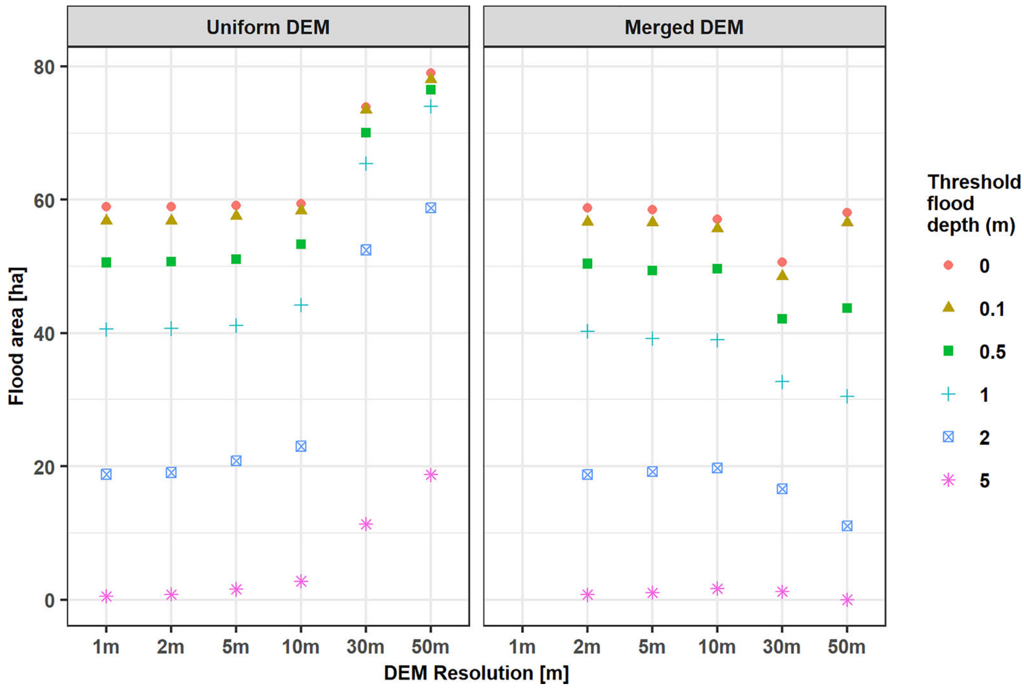

Fig. 14. Flooded area vs DEM resolution for both uniform and merged DEMs for threshold flood depths ranging from 0 to 50 m.

Table 2
Total flood area and mean flood depth derived from DEMs with different resolution and configuration.

DEM Resolution (m)	Flooded area (ha)		Mean flood depth (m)	
	Uniform	Merged	Uniform	Merged
1 (Benchmark)	58.9		1.74	
2	59.0	58.8	1.77	1.76
5	59.2	58.5	1.85	1.80
10	59.4	57.1	2.01	1.90
30	73.9	50.6	3.30	1.81
50	79.0	58.0	4.30	1.38

from 1 m to 50 m increases the simulated total flooded area from 58.9 ha to 79.0 ha (30%). The effect caused by the loss of the characterisation of the river channel can again be seen when the uniform DEM resolution decreases from 10 m to 30 m. The simulated flooded area increases marginally from 58.9 ha to 59.4 ha when the DEM resolution decreases from 1 m to 10 m. However, it increases from 59.4 ha to 73.9 ha when the DEM resolution decreases from 10 m to 30 m. With merged DEMs, as we already observed in Fig. 12, the difference in the simulated flooded area is much less and without a consistent pattern. In fact, the total flooded area with a 10 m resolution DEM of 57.1 ha is greater than the flooded area of 50.6 ha with a 30 m resolution DEM regardless of the threshold flood depth.

3.4. Error estimation

To estimate the error caused by the use of a coarser resolution in both uniform and merged DEMs, the overall root mean square error (RMSE) was calculated for predicted flood depths for all the resolutions, against the reference case (Fig. 15). The flood depths in all the individual cells that were flooded in the reference case were used for this calculation. This is a commonly used simple measure to calculate the error in 2D flood modelling (Ogania et al., 2019; Ozdemir et al., 2013; Saksena and Merwade, 2015a). In our case, flood predictions with uniform DEMs show an increasing linear trend against RMSE. Saksena and Merwade (2015a) also found an increasing linear trend of RMSE against grid size,

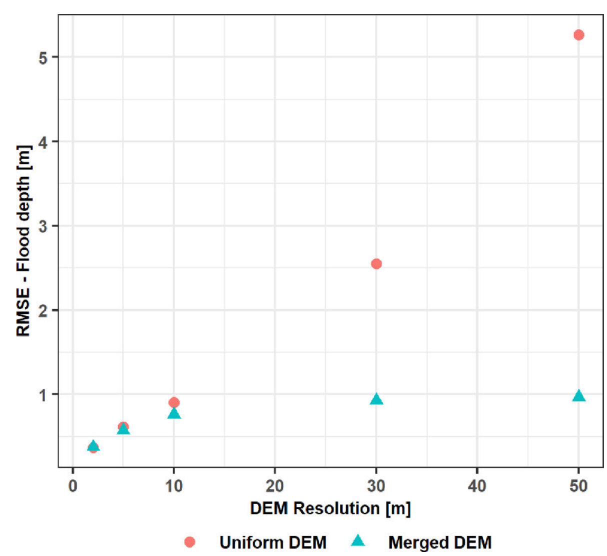

Fig. 15. RMSE vs DEM resolution for both uniform and merged DEMs.

which agrees with our findings.

When merged DEMs are used, there is a significant reduction in the estimated error, with the RMSE reducing from 2.6 m to 0.9 m at 30 m resolution and from 5.25 m to 1 m at 50 m resolution. It is interesting to note that for a DEM resolution up to 10 m, the improvement is not significant. This is because the loss of river channel characterisation is not very apparent until the DEM resolution goes above 10 m (in this case). This will, of course, be dependent on the width of the river channel.

Fig. 16 shows the fit index variation, which provides a measure of the error in terms of the predicted flood extent with reference to the reference flood map obtained using 1 m DEM. The fit index shows a progressive reduction in the agreement with the reference case as the resolution decreases from 1 m to 50 m with a 25% reduction with a 50 m resolution uniform DEM. To understand whether this due to false

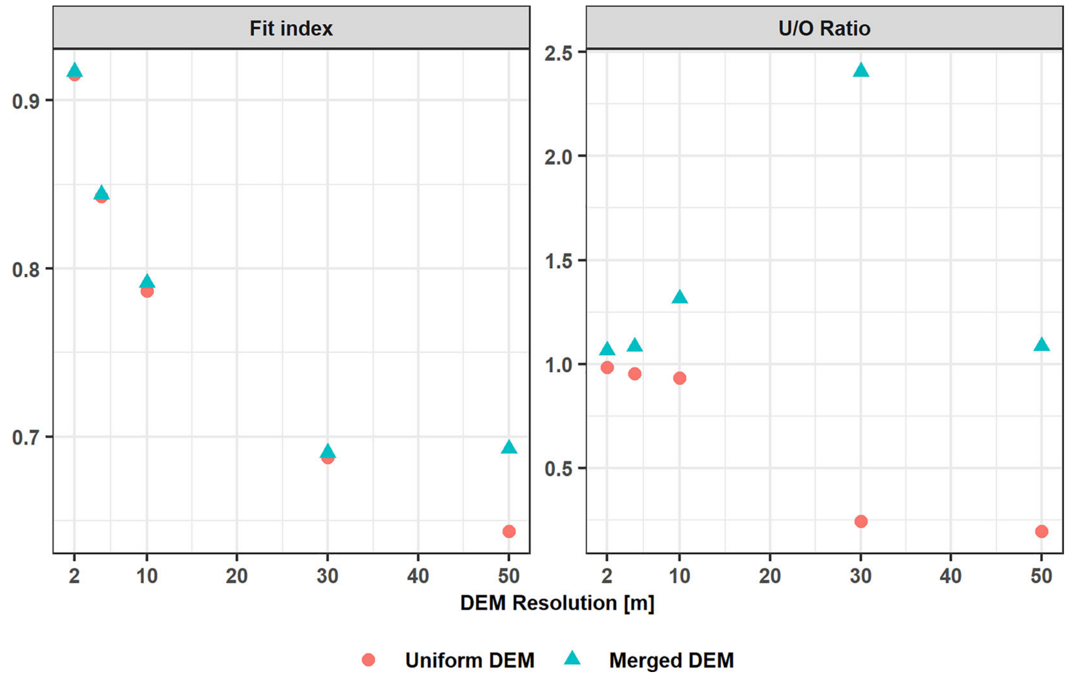

Fig. 16. Fit index and U/O (underprediction/overprediction) ratio for both uniform and merged DEMs.

positives (overestimation) or false negatives (underestimation) the ratio between overestimation/underestimation is also presented in Fig. 16 (U/O ratio). This ratio is always less than one for uniform DEM flood maps which indicates that there is a greater degree of overestimation in the modelled results. However, it is interesting to note that underestimation also occurs where the lower resolution flood models failed to predict certain flooded areas. This is likely to be where the coarser-resolution DEMs result in certain cells increasing in height thereby reducing flood propagation. With merged DEMs, again the changes up to 10 m resolution are not as significant as the resolutions greater than 10 m. Although the fit index did not show a significant difference with the 30 m resolution DEM, it is clear from the U/O ratio that it is due to underprediction of the flooded area with a merged DEM. Interestingly, flood maps derived with merged DEMs underpredict the flooded area compared with uniform DEMs, which always over predict. This demonstrates that it is the effect of the river channel characterisation that results in the overprediction of flood area and depth when using coarser resolution DEMs. Without the loss of characterisation of the river channel, the common perception of overprediction due to coarser resolution is not always true. In addition, the absence of a consistent trend in the U/O ratio for merged DEMs indicates that it is largely dependent on the modelled terrain.

3.5. General discussion

There was no clear pattern in the changes in elevation of the land cells when coarser-resolution DEMs were used, as many land cells were raised as were lowered. However, there was an increase in flood depths of 80–90% for the land cells when using the coarser-resolution DEM ranging from 2 m to 50 m compared with the 1 m resolution DEM reference case. This is due to the loss of characterisation of the river channel, including an apparent raising of the river bed as the DEM resolution decreases resulting in more water being propagated from the river cells into the surrounding land cells. This finding was corroborated by the use of merged DEMs in which the characterisation of the river channel remains the same throughout and a. there was no consistent trend of overestimation or underestimation in flood depths and extents and b. there was a better agreement between the modelled flood depths and extents and the reference case compared with uniform DEMs. It is clear that the river width has to be one of the deciding factors when considering the optimal resolution of DEM to be used when carrying out a fluvial flood model for a particular location. As observed once the DEM resolution exceeds the river width, the overprediction of flood depth and extent increase significantly. The change in the simulated flooded area, resulting from the 15 m wide River Cocker and the 50 m wide River Derwent, as the DEM resolution decreased from 10 m to 30 m, was 30 times higher than the change in the flooded area when the DEM resolution decreased from 1 m to 10 m. This demonstrates that the resolution of the DEM used to characterise the river channel should be at least less than the river width.

Although the use of a coarser resolution DEM results overall in an overprediction of flood depths and extents, there are river stretches where there are reduced flood depths due to the use of coarser-resolution DEMs. These are locations where the surrounding area is low lying without much urban development to confine the flood water to the river. This finding helps to identify river stretches where a coarser resolution DEM would possibly under or over-predict flood depths. Such knowledge would be of great value if flood management decisions need to be taken using a flood map produced using a coarser resolution DEM.

The availability of fit for purpose data and the national significance of the Storm Desmond flood event were the main reasons for the choice of the case study. We believe this study area, with a large proportion of built-up area (Fig. 1), represents a typical urban surface. Furthermore, since the lowest resolution used in this study was 1 m, it was a preferable choice to use a small urban area as it allowed us to study the effect of different resolution DEMs in detail and understand better the local influences on the DEM and the consequent flood behaviour. Similar studies in the past also took advantage of relatively small study areas which enabled them to understand the local dynamics better (Leitão et al., 2016; Ozdemir et al., 2013). For example, Ozdemir et al. (2013) used a study area of 0.1 km^2 (10 ha) for their study to look at the effect of DEM resolutions ranging from 10 cm to 1 m. Leitão et al. (2016) used an area of 0.9 km^2 to assess the impact of combining different DEMs on flood modelling results. Although the values of the comparators could be different for another study area with a smaller or larger urban area, the major finding is still valid which is, there is a significant improvement in the prediction of flood properties when a DEM of sufficient resolution is used to define adequately the riverbed that is then used within a 2D

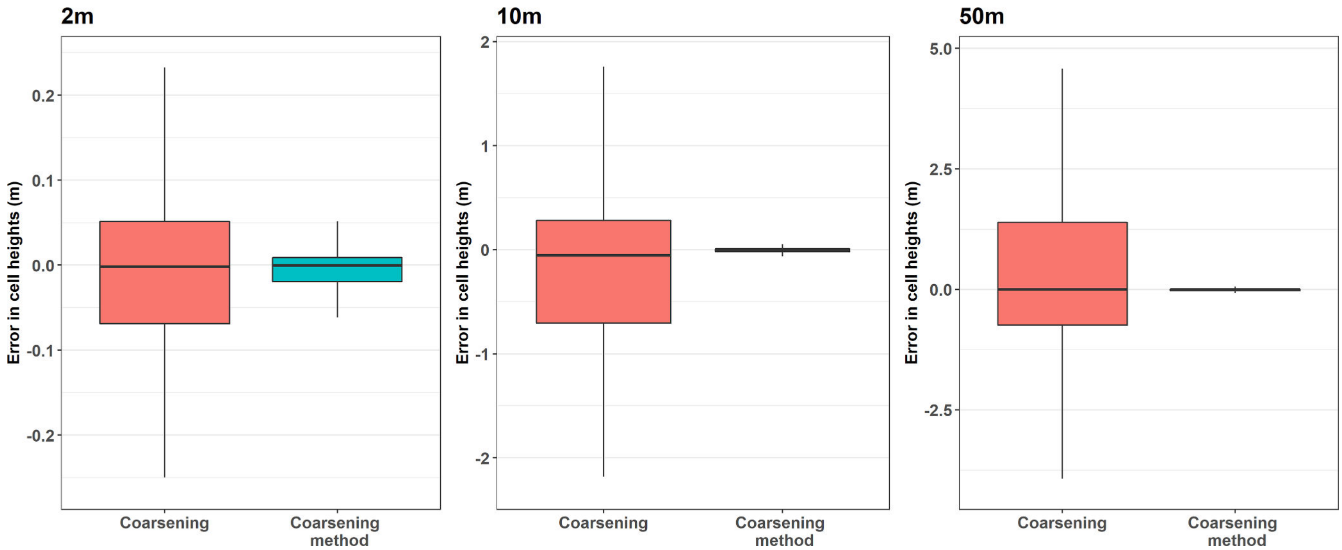

Fig. 17. The effect of coarsening method in resampled DEM cell heights in comparison to the resampled error.

fluvial model.

In this study, we have used bilinear interpolation for resampling. This is one of the most commonly used methods for DEM resampling (ESRI, 2020). The other most commonly used resampling method is cubic convolution interpolation. It has been shown in the past that the resampling method can have an impact on the resulting DEMs (Aguilar et al., 2005; Chaplot et al., 2006; Heritage et al., 2009). However, we do not expect the impact of the coarsening method to be significant in comparison to the coarsening effect itself, especially at resolutions coarser than 10 m where the coarsening effects are very significant. To assess this, we compared the effect of coarsening with the effect of the coarsening method for 2 m, 10 m, and 50 m resolution DEMs. We compared bilinear interpolation (the one used in this study) with cubic convolution interpolation (Keys, 1981). We did not test the nearest neighbour approach for DEM resampling as it is primarily used for discrete data (ESRI, 2020). The nearest neighbour approach will also result in a rougher DEM surface which is then likely to cause instabilities in the flood model, especially at resolutions coarser than 10 m. Fig. 17 shows the boxplot of errors caused by coarsening (with reference to the 1 m DEM) and the boxplot of differences between the cell heights obtained using the different resampling methods (bilinear interpolation and cubic convolution interpolation) for 2 m, 10 m and 50 m resolution DEMs. As can be seen from the plots, the difference in cell heights using the two different methods is almost negligible compared to the error caused by the coarsening at resolutions of 10 m and 50 m. Although at 2 m resolution the sampling effect is greater, it still considerably less than the differences caused by the coarsening effect. In addition, the aim of the study was to demonstrate the advantage of merged DEMs over coarser resolution DEMS, where this effect is negligible.

Due to the scope of this study, we kept the mesh size constant for all the simulations, so there was no significant change in the computational time. However, in other situations, the size of the computational mesh will be based on the DEM resolution. The coarser the DEM resolution, the larger the computational mesh size will be. This will significantly reduce the computational burden and can be utilised in modelling applications such as flood warning systems.

In this study, we have not addressed issues that arise from DEM errors during measurement and post-processing. However, we acknowledge the fact that depending the techniques used, these errors could be as significant as coarsening errors (Abily et al., 2016; Wang et al., 2012; Zotou et al., 2020). Further, recent studies have also raised the issue of the “blocking-out” effect of buildings in DTMs which prevent flood flows and possible storage effects of the buildings in flood modelling (Bellos and Tsakiris, 2015). We believe, in future in addition to DEM and mesh configurations, this also needs to be studied in detail in 2D flood modelling given its potential impact on the flood dynamics in a built-up area.

4. Conclusion

This study, first, investigates the root causes of the impact of DEM resolution on urban fluvial flood modelling using DEMs ranging from 1 m to 50 m. DEMs with resolutions of 2 m to 50 m were derived by resampling the 1 m DEM. The study then investigates how DEM resolution affects the definition and characterisation of the river channel and the consequences of this for the modelled results. For this purpose, a separate set of merged DEMs were generated where the river channel obtained with the 1 m resolution DEM is merged with coarser resolution DEMs. Data obtained during the flood event caused by Storm Desmond (2015) in Cockermouth (Cumbria, UK) was used for this study. The study area covers around 142 ha with the town centre located at the confluence of two rivers – the River Derwent and the River Cocker. The HEC-RAS 2D model was used for all the simulations. The benchmark model obtained with the 1 m resolution DEM was calibrated with measured water levels at two locations within the rivers.

The following conclusions can be made from the results

- The use of coarser-resolution DEMs in the model affected river cells in a different way to the land cells. Within the river channel the coarser-resolution DEMs raised more cells than it lowered. When using a 2 m resolution DEM, 53% of cells were raised and 47% lowered. However, when using a 50 m resolution DEM 91% were raised and 9% lowered. For the land cells, there was less of an effect with the ratio between raising and lowering the ratio was between 0.9 and 1.7 at different DEM resolutions.
- Overall, the flood depth and flood extent increased with decreasing DEM resolution. There was a 30% increase in flood extent from 58.9 ha to 79.0 ha and a 150% increase in mean flood depth from 1.74 m to 4.30 m when the DEM resolution reduces from 1 m grid to 50 m grid. The main reason for this is the increasing lack of definition of the river channel with an associated reduction in the estimated depth of the river resulting in reduced river channel conveyance. This then leads to an increase in the flood extent and depth especially in the immediate vicinity of the river.
- Despite the overall over prediction of flood depths due to the use of a coarser resolution DEM, there were also areas both inside and

outside of the river channel where the flood depth was under predicted. The main reason being the increased elevation of these areas due to the use of a coarser resolution DEM.

- In river stretches where there are no developments or there are lower river banks, the flood water propagates into the surrounding areas when using coarser resolution DEMs. This consequently reduces the flood depth of the river cells at these river stretches. This means the coarser-resolution DEM does not always increase the flood depth everywhere within the river. The land use and terrain of the surrounding area also have an associated effect.
- When the river channel is characterised using a high-resolution DEM and is then used in conjunction with a coarser resolution DEM for the surrounding area (merged DEMs), there is a significant improvement in the agreement between the modelled and the actual results of flood depths. The use of merged DEMs reduced the error in mean flood depth from 150% to 20% and the overall RMSE in flood depths from 5.26 m to 0.98 m at 50 m resolution. However, there is no consistent trend in the RMSE with the resolution of the merged DEM. This is different to the findings with the uniform DEM where the RMSE increases linearly with the resolution.
- In terms of flood extent, the use of coarser-resolution merged DEMs tend to underpredict the affected area compared with uniform DEMs. However, the Fit Index comparison demonstrates that merged DEMs provide a better indication of flood extent than uniform DEMs.
- It is clear that the resolution of the DEM used has an impact on the simulated flood extents and depths. For optimal results, the resolution of the DEM used for a particular location should be at least finer than the width of the river channel.

We have demonstrated that the use of merged DEMs may be a cost-effective way of obtaining fit for purpose flood maps in locations where high resolution DEMs have not yet been developed. The use of merged DEMs significantly improves the flood prediction in comparison to uniform DEMs. This could help improve flood modelling without having to survey the entire model extent when there are financial and practical limitation, which is often the case especially in developing countries. For example, NASA's Shuttle Radar Topography Mission DEMs, which are 30 m resolution, are freely available. However, when this DEM is used in a fluvial flood model, the resulting flood depths and flood extents could be significantly higher (or sometimes lower) depending on factors such the widths of river channels, the degree of urbanisation and the topography of the surrounding areas. This study suggests that using the SRTM DEMs together with a better representation of the river channel derived from bathymetry or a higher resolution DEM (e.g. 1 m) might be a more cost-effective approach than seeking to obtain a high-resolution DEM for the whole area. In addition, there may not be the resources available to generate a wide-scale 1 m resolution DEM. Our findings also have implications for other flood risk management activities such as the identification of emergency evacuation routes. The approach we have developed provides a means of developing reliable flood risk maps without necessarily requiring a high resolution DEM for the total affected area. Such maps can then inform the development of better overall flood risk management practices.

CRediT authorship contribution statement

Manoranjan Muthusamy: Conceptualization, Data curation, Methodology, Validation, Writing - original draft, Writing - review & editing. **Mónica Rivas Casado:** Conceptualization, Data curation, Methodology, Validation, Writing - original draft, Writing - review & editing, Supervision, Funding acquisition. **David Butler:** Validation, Writing - review & editing, Supervision, Funding acquisition. **Paul Leinster:** Validation, Writing - review & editing, Supervision, Funding acquisition.

Declaration of Competing Interest

The authors declare that they have no known competing financial interests or personal relationships that could have appeared to influence the work reported in this paper.

Acknowledgement

This research was funded by EPSRC, EP/P02839X/1 "Emergency flood planning and management using unmanned aerial systems". Data underlying this study can be accessed through the Cranfield University repository at: https://doi.org/10.17862/cranfield.rd.12221204.

References

Abily, M., Bertrand, N., Delestre, O., Gourbesville, P., Duluc, C.M., 2016. Spatial Global Sensitivity Analysis of High Resolution classified topographic data use in 2D urban flood modelling. Environ. Model. Softw. 77, 183–195. https://doi.org/10.1016/j.envsoft.2015.12.002.

Aguilar, F.J., Agüera, F., Aguilar, M.A., Carvajal, F., 2005. Effects of terrain morphology, sampling density, and interpolation methods on grid DEM accuracy. Photogramm. Eng. Remote Sensing 71, 805–816. https://doi.org/10.14358/PERS.71.7.805.

Arcement, G.J., Schneider, V.R., 1989. Guide for Selecting Manning's Roughness Coefficients for Natural Channels and Flood Plains.

Aronica, G., Bates, P.D., Horritt, M.S., 2002. Assessing the uncertainty in distributed model predictions using observed binary pattern information within GLUE. Hydrol. Process. 16, 2001–2016. https://doi.org/10.1002/hyp.398.

Azizian, A., Brocca, L., 2020. Determining the best remotely sensed DEM for flood inundation mapping in data sparse regions. Int. J. Remote Sens. 41, 1884–1906. https://doi.org/10.1080/01431161.2019.1677968.

Bates, P.D., 2012. Integrating remote sensing data with flood inundation models: how far have we got? Hydrol. Process. 26, 2515–2521. https://doi.org/10.1002/hyp.9374.

Bates, P.D., 2004. Remote sensing and flood inundation modelling. Hydrol. Process. 18, 2593–2597. https://doi.org/10.1002/hyp.5649.

Bellos, V., Tsakiris, G., 2015. Comparing Various Methods of Building Representation for 2D Flood Modelling In Built-Up Areas. Water Resour. Manag. 29, 379–397. https://doi.org/10.1007/s11269-014-0702-3.

Brandt, S.A., 2016. Modeling and visualizing uncertainties of flood boundary delineation: algorithm for slope and DEM resolution dependencies of 1D hydraulic models. Stoch. Environ. Res. Risk Assess. 30, 1677–1690. https://doi.org/10.1007/s00477-016-1212-z.

Chaplot, V., Darboux, F., Bourennane, H., Leguédois, S., Silvera, N., Phachomphon, K., 2006. Accuracy of interpolation techniques for the derivation of digital elevation models in relation to landform types and data density. Geomorphology 77, 126–141. https://doi.org/10.1016/j.geomorph.2005.12.010.

Chow, V.T., 1959. Open Channel Hydraulics. McGraw-Hill, New York.

Corringham, T.W., Cayan, D.R., 2019. The Effect of El Niño on flood damages in the Western United States. Weather. Clim. Soc. 11, 489–504. https://doi.org/10.1175/WCAS-D-18-0071.1.

Environment Agency, 2018. Environment Agency - Data [WWW Document]. URL <https://data.gov.uk/search?filters%5Bpublisher%5D=Environment+Agency> (accessed 4.1.18).

Environment Agency, 2009. Flooding in England: A National Assessment of Flood Risk.

ESRI, 2020. ArcGIS Pro help [WWW Document]. URL <https://pro.arcgis.com/en/pro-app/help/main/welcome-to-the-arcgis-pro-app-help.htm> (accessed 12.9.20).

Heritage, G.L., Milan, D.J., Large, A.R.G., Fuller, I.C., 2009. Influence of survey strategy and interpolation model on DEM quality. Geomorphology 112, 334–344. https://doi.org/10.1016/j.geomorph.2009.06.024.

Horritt, M.S., Bates, P.D., 2001. Effects of spatial resolution on a raster based model of flood flow. J. Hydrol. 253, 239–249.

Jung, H.C., Jasinski, M., Kim, J.-W., Shum, C.K., Bates, P., Neal, J., Lee, H., Alsdorf, D., 2012. Calibration of two-dimensional floodplain modeling in the central Atchafalaya Basin Floodway System using SAR interferometry. Water Resour. Res. 48 https://doi.org/10.1029/2012WR011951.

Keys, R., 1981. Cubic convolution interpolation for digital image processing. IEEE Trans. Acoust. 29, 1153–1160. https://doi.org/10.1109/TASSP.1981.1163711.

Leitão, J.P., Moy De Vitry, M., Scheidegger, A., Rieckermann, J., 2016. Assessing the quality of digital elevation models obtained from mini unmanned aerial vehicles for overland flow modelling in urban areas. Hydrol. Earth Syst. Sci. 20, 1637–1653. https://doi.org/10.5194/hess-20-1637-2016.

Met Office, 2018. UK STORM CENTRE [WWW Document]. URL <https://www.metoffice.gov.uk/barometer/uk-storm-centre> (accessed 11.16.18).

Office for National Statistics, 2018. Local statistics - Office for National Statistics [WWW Document]. URL <https://www.ons.gov.uk/help/localstatistics> (accessed 11.16.18).

Ogania, J.L., Puno, G.R., Alivio, M.B.T., Taylaran, J.M.G., 2019. Effect of digital elevation model's resolution in producing flood hazard maps. Glob. J. Environ. Sci. Manag. 5, 95–106. https://doi.org/10.22034/gjesm.2019.01.08.

Ozdemir, H., Sampson, C.C., de Almeida, G.A.M., Bates, P.D., 2013. Evaluating scale and roughness effects in urban flood modelling using terrestrial LIDAR data. Hydrol. Earth Syst. Sci. 17, 4015–4030. https://doi.org/10.5194/hess-17-4015-2013.

Pappenberger, F., Frodsham, K., Beven, K., Romanowicz, R., Matgen, P., 2007. Fuzzy set approach to calibrating distributed flood inundation models using remote sensing observations. Hydrol. Earth Syst. Sci. 11, 739–752. https://doi.org/10.5194/hess-11-739-2007.

Peña, F., Nardi, F., 2018. Floodplain terrain analysis for coarse resolution 2D flood modeling. Hydrology 5. https://doi.org/10.3390/hydrology5040052.

Pottier, N., Penning-Rowsell, E., Tunstall, S., Hubert, G., 2005. Land use and flood protection: contrasting approaches and outcomes in France and in England and Wales. Appl. Geogr. 25, 1–27. https://doi.org/10.1016/j.apgeog.2004.11.003.

Saksena, S., Merwade, V., 2015. Incorporating the effect of DEM resolution and accuracy for improved flood inundation mapping. J. Hydrol. 530, 180–194. https://doi.org/10.1016/j.jhydrol.2015.09.069.

Schumann, G., Bates, P.D., Horritt, M.S., Matgen, P., Pappenberger, F., 2009. Progress in integration of remote sensing–derived flood extent and stage data and hydraulic models. Rev. Geophys. 47 https://doi.org/10.1029/2008RG000274.

Schumann, G., Matgen, P., Hoffmann, L., Hostache, R., Pappenberger, F., Pfister, L., 2007. Deriving distributed roughness values from satellite radar data for flood inundation modelling. J. Hydrol. 344, 96–111. https://doi.org/10.1016/j.jhydrol.2007.06.024.

Tamiru, A., Rientjes, T.H.M., 2005. Effects of lidar dem resolution in flood modelling: a model sentitivity study for the city of Tegucigalpa, Honduras, in: ISPRS WG III/3, III/4, V/3 Workshop "Laser Scanning 2005." pp. 168–173.

Thomas Steven Savage, J., Pianosi, F., Bates, P., Freer, J., Wagener, T., 2016. Quantifying the importance of spatial resolution and other factors through global sensitivity analysis of a flood inundation model. Water Resour. Res. 52, 9146–9163. https://doi.org/10.1002/2015WR018198.

U.S. Army Corps of Engineering, 2016. HEC-RAS 5.0 Hydraulic Reference Manual. U.S. Army Corps of Engineers, Institute for Water Resources, Hydrologic Engineering Center, Davis, CA, USA. CPD-68.

Wang, W., Yang, X., Yao, T., 2012. Evaluation of ASTER GDEM and SRTM and their suitability in hydraulic modelling of a glacial lake outburst flood in southeast Tibet. Hydrol. Process. 26, 213–225. https://doi.org/10.1002/hyp.8127.

Ward, P.J., Jongman, B., Kummu, M., Dettinger, M.D., Sperna Weiland, F.C., Winsemius, H.C., 2014. Strong influence of El Niño Southern Oscillation on flood risk around the world. Proc. Natl. Acad. Sci. U. S. A. 111, 15659–15664. https://doi.org/10.1073/pnas.1409822111.

Werner, M., Blazkova, S., Petr, J., 2005. Spatially distributed observations in constraining inundation modelling uncertainties. Hydrol. Process. 19, 3081–3096. https://doi.org/10.1002/hyp.5833.

WHO, 2020. World Health Organisation - Flood [WWW Document]. URL <https://www.who.int/health-topics/floods#tab=tab_2> (accessed 4.29.20).

Zotou, I., Bellos, V., Gkouma, A., Karathanassi, V., Tsihrintzis, V.A., 2020. Using sentinel-1 imagery to assess predictive performance of a hydraulic model. Water Resour. Manag. 34, 4415–4430. https://doi.org/10.1007/s11269-020-02592-7.